Parallel three-dimensional simulations of quasi-static elastoplastic solids

Nicholas M. Boffi & Chris Rycroft

July 16, 2019

Harvard University, Department of Applied Mathematics.
CSGF Program Review 2019.

Bulk metallic glasses (BMGs)

Graph taken from Maas, Loffler, *Adv. Func. Mater.* 2015, 25, 2353-2368.

Bulk metallic glasses (BMGs)

- Solid material held together by metallic bonds with an amorphous atomic-scale structure.

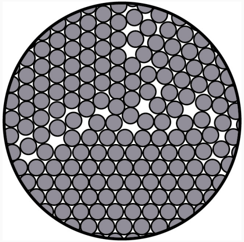

Crystalline structure

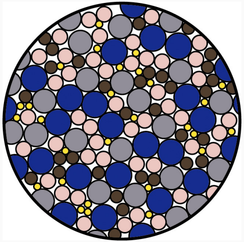

Amorphous structure

Graph taken from Maas, Loffler, *Adv. Func. Mater.* 2015, 25, 2353-2368.

Bulk metallic glasses (BMGs)

- Solid material held together by metallic bonds with an amorphous atomic-scale structure.
- Metallic bonds lead to dense packing unlike oxide glasses.
  - Stronger than steel, with high strength to elasticity ratio.
  - Can be processed and molded like a plastic.

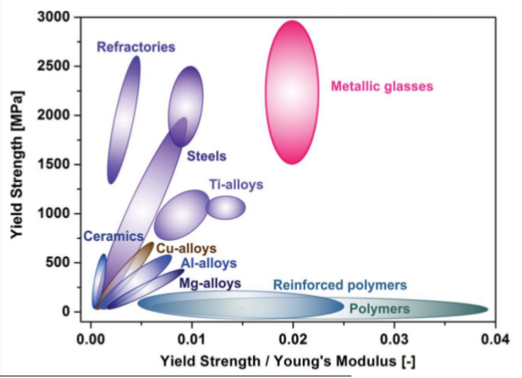

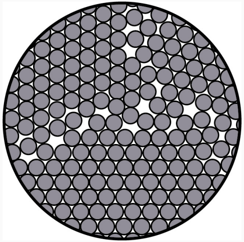

Crystalline structure

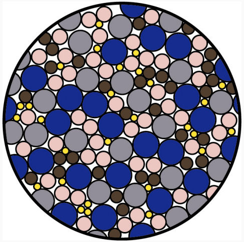

Amorphous structure

Graph taken from Maas, Loffler, *Adv. Func. Mater.* 2015, 25, 2353-2368.

Bulk metallic glasses (BMGs)

- Solid material held together by metallic bonds with an amorphous atomic-scale structure.
- Metallic bonds lead to dense packing unlike oxide glasses.
    - Stronger than steel, with high strength to elasticity ratio.
    - Can be processed and molded like a plastic.
- Applications limited by catastrophic failure mechanism: shear banding.

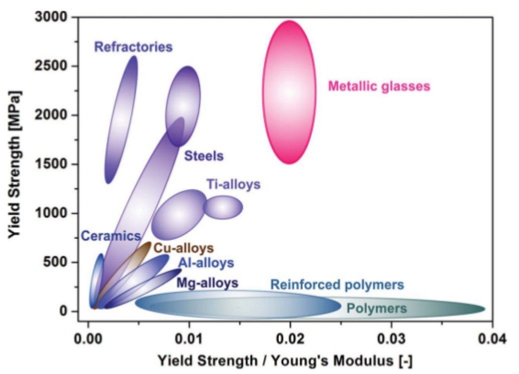

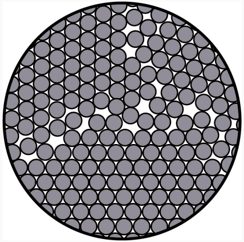

Crystalline structure

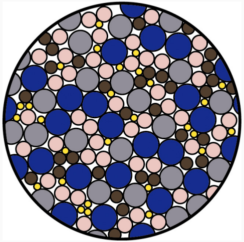

Amorphous structure

Graph taken from Maas, Loffler, *Adv. Func. Mater.* 2015, 25, 2353-2368.

Shear bands

Images taken from Schroers & Johnson, *Phys. Rev. Let.*, 2004, 93, 255506

Shear bands

- Shear band: rapid (ms) narrow (10 nm) localization of plastic deformation due to a strain-softening instability.

Images taken from Schroers & Johnson, *Phys. Rev. Let.*, 2004, 93, 255506

Shear bands

- Shear band: rapid (ms) narrow (10 nm) localization of plastic deformation due to a strain-softening instability.

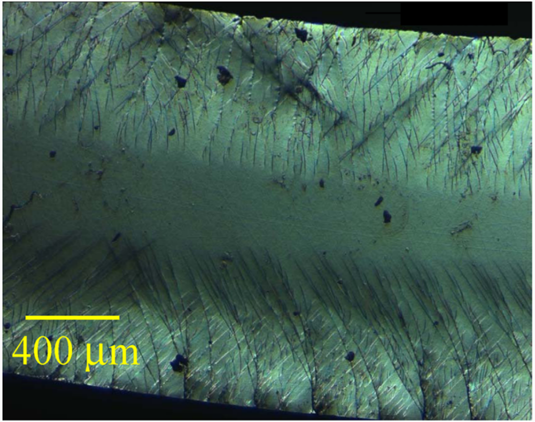

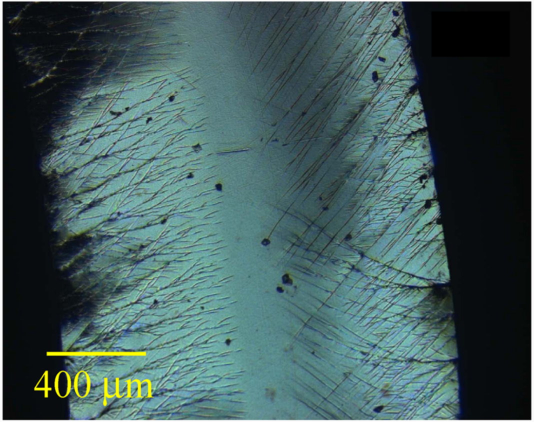

Images taken from Schroers & Johnson, *Phys. Rev. Let.*, 2004, 93, 255506

Shear bands

- Shear band: rapid (ms) narrow (10 nm) localization of plastic deformation due to a strain-softening instability.
- Physics: Any theory of amorphous plasticity must be able to predict structure and formation of shear bands.

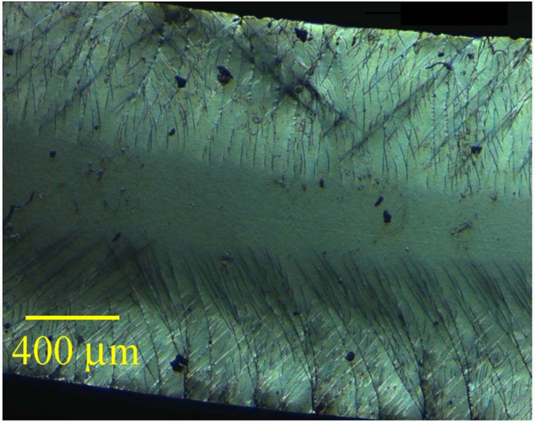

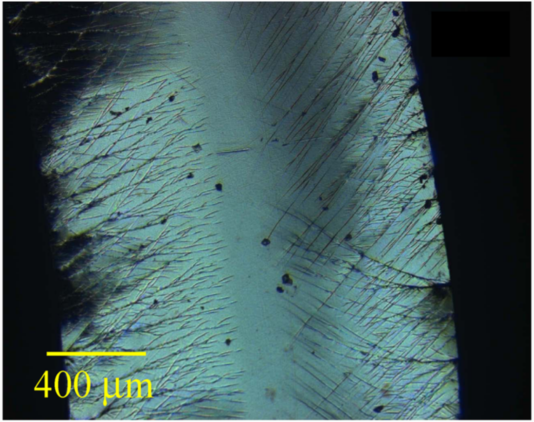

Images taken from Schroers & Johnson, *Phys. Rev. Let.*, 2004, 93, 255506

Shear bands

- Shear band: rapid (ms) narrow (10 nm) localization of plastic deformation due to a strain-softening instability.
- Physics: Any theory of amorphous plasticity must be able to predict structure and formation of shear bands.
- Applications: Until shear bands are understood and controlled, BMGs cannot be used in practice.

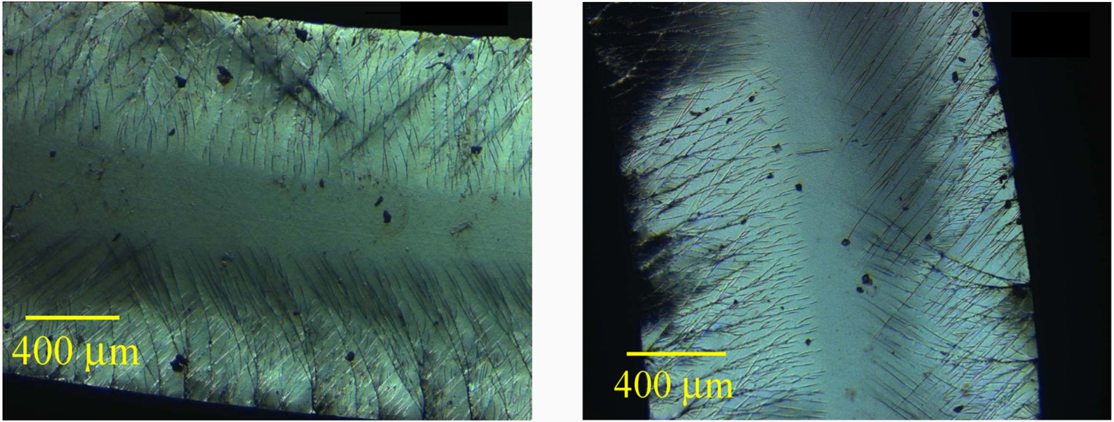

Images taken from Schroers & Johnson, *Phys. Rev. Let.*, 2004, 93, 255506

Shear transformation zone theory of amorphous plasticity

Images taken from K. Kamrin, E. Bouchbinder, *J. Mech. Phys. Solids* 73 (2014) 269-288 and Greer, Cheng, & Ma, *Mat. Sci. Eng. R* 74 (2013) 71-132.

Shear transformation zone theory of amorphous plasticity

- STZs: localized regions likely to undergo small-scale plastic rearrangements.

Images taken from K. Kamrin, E. Bouchbinder, *J. Mech. Phys. Solids* 73 (2014) 269-288 and Greer, Cheng, & Ma, *Mat. Sci. Eng. R* 74 (2013) 71-132.

Shear transformation zone theory of amorphous plasticity

- STZs: localized regions likely to undergo small-scale plastic rearrangements.

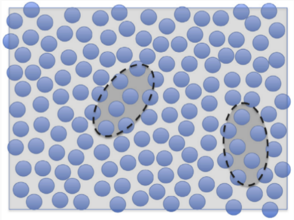

Images taken from K. Kamrin, E. Bouchbinder, *J. Mech. Phys. Solids* 73 (2014) 269-288 and Greer, Cheng, & Ma, *Mat. Sci. Eng. R* 74 (2013) 71-132.

Shear transformation zone theory of amorphous plasticity

- STZs: localized regions likely to undergo small-scale plastic rearrangements.

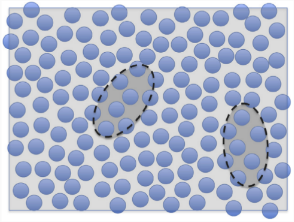

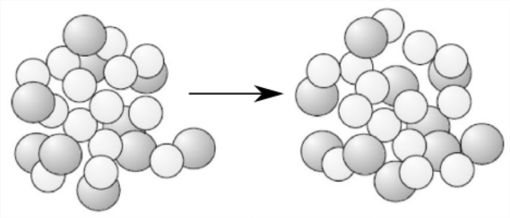

Images taken from K. Kamrin, E. Bouchbinder, *J. Mech. Phys. Solids* 73 (2014) 269-288 and Greer, Cheng, & Ma, *Mat. Sci. Eng. R* 74 (2013) 71-132.

Shear transformation zone theory of amorphous plasticity

- STZs: localized regions likely to undergo small-scale plastic rearrangements.
- Randomly distributed with Boltzmann density in an effective disorder temperature χ.

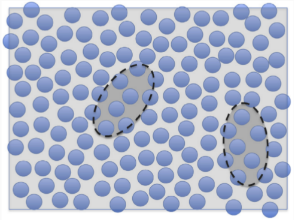

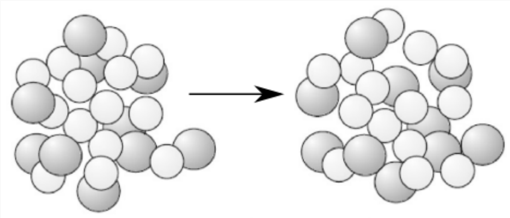

Images taken from K. Kamrin, E. Bouchbinder, *J. Mech. Phys. Solids* 73 (2014) 269-288 and Greer, Cheng, & Ma, *Mat. Sci. Eng. R* 74 (2013) 71-132.

Shear transformation zone theory of amorphous plasticity

- STZs: localized regions likely to undergo small-scale plastic rearrangements.
- Randomly distributed with Boltzmann density in an effective disorder temperature χ.
- χ is measured in Kelvin, $\chi \propto \frac{\partial(\text{Config. Energy})}{\partial(\text{Config. Entropy})}$, but distinct from usual kinetic/vibrational temperature T.

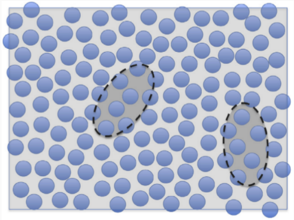

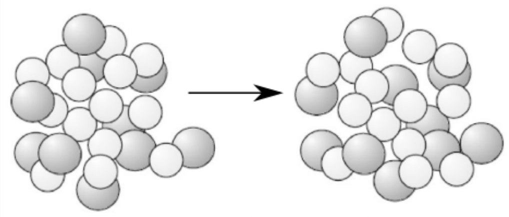

Images taken from K. Kamrin, E. Bouchbinder, *J. Mech. Phys. Solids* 73 (2014) 269-288 and Greer, Cheng, & Ma, *Mat. Sci. Eng. R* 74 (2013) 71-132.

Continuum theory

Linear Elasticity

Shear Transformation Zone Theory

Continuum theory

Linear Elasticity

$$\underbrace{\frac{\mathcal{D}\sigma}{\mathcal{D}t}}_{\text{Truesdell Rate}} = \overbrace{\mathbf{C}}^{\text{Stiffness}} : \underbrace{\mathbf{D}^{\text{el}}}_{\text{Elastic Part}}$$

Shear Transformation Zone Theory

Continuum theory

Linear Elasticity

$$\underbrace{\frac{\mathcal{D}\sigma}{\mathcal{D}t}}_{\text{Truesdell Rate}} = \overbrace{\mathbf{C}}^{\text{Stiffness}} : \underbrace{\mathbf{D}^{\text{el}}}_{\text{Elastic Part}}$$

$$\underbrace{\mathbf{D}}_{\text{Rate of deformation}} = \underbrace{\frac{1}{2}(\nabla\mathbf{u} + (\nabla\mathbf{u})^T)}_{\text{Definition}}$$

Shear Transformation Zone Theory

Continuum theory

Linear Elasticity

$$\underbrace{\frac{\mathcal{D}\sigma}{\mathcal{D}t}}_{\text{Truesdell Rate}} = \overbrace{\mathbf{C}}^{\text{Stiffness}} : \underbrace{\mathbf{D}^{\text{el}}}_{\text{Elastic Part}}$$

$$\underbrace{\mathbf{D}}_{\text{Rate of deformation}} = \underbrace{\frac{1}{2}(\nabla\mathbf{u} + (\nabla\mathbf{u})^T)}_{\text{Definition}}$$

$$= \underbrace{\mathbf{D}^{el} + \mathbf{D}^{pl}}_{\text{hypo-elastoplastic assumption}}$$

Shear Transformation Zone Theory

Linear Elasticity

$$\underbrace{\frac{\mathcal{D}\sigma}{\mathcal{D}t}}_{\text{Truesdell Rate}} = \overbrace{\mathbf{C}}^{\text{Stiffness}} : \underbrace{\mathbf{D}^{\text{el}}}_{\text{Elastic Part}}$$

$$\underbrace{\mathbf{D}}_{\text{Rate of deformation}} = \underbrace{\frac{1}{2}(\nabla\mathbf{u} + (\nabla\mathbf{u})^T)}_{\text{Definition}}$$

$$= \underbrace{\mathbf{D}^{el} + \mathbf{D}^{pl}}_{\text{hypo-elastoplastic assumption}}$$

$$\underbrace{\rho\frac{d\mathbf{u}}{dt}}_{m \times a} = \underbrace{\nabla \cdot \sigma}_{\text{Net force}}$$

Shear Transformation Zone Theory

Continuum theory

Linear Elasticity

$$\underbrace{\frac{\mathcal{D}\sigma}{\mathcal{D}t}}_{\text{Truesdell Rate}} = \overbrace{\mathbf{C}}^{\text{Stiffness}} : \underbrace{\mathbf{D}^{\text{el}}}_{\text{Elastic Part}}$$

$$\underbrace{\mathbf{D}}_{\text{Rate of deformation}} = \underbrace{\frac{1}{2}(\nabla \mathbf{u} + (\nabla \mathbf{u})^T)}_{\text{Definition}}$$

$$= \underbrace{\mathbf{D}^{el} + \mathbf{D}^{pl}}_{\text{hypo-elastoplastic assumption}}$$

$$\underbrace{\rho \frac{d\mathbf{u}}{dt}}_{m \times a} = \underbrace{\nabla \cdot \sigma}_{\text{Net force}}$$

Shear Transformation Zone Theory

$$\underbrace{\mathbf{D}^{pl}}_{\text{Plastic rate}} = \underbrace{D^{pl} f(\sigma)}_{\propto \text{ deviatoric}}$$

Continuum theory

Linear Elasticity

$$\underbrace{\frac{\mathcal{D}\sigma}{\mathcal{D}t}}_{\text{Truesdell Rate}} = \overbrace{\hat{\mathbf{C}}}^{\text{Stiffness}} : \underbrace{\mathbf{D}^{\text{el}}}_{\text{Elastic Part}}$$

$$\underbrace{\mathbf{D}}_{\text{Rate of deformation}} = \underbrace{\frac{1}{2}(\nabla\mathbf{u} + (\nabla\mathbf{u})^T)}_{\text{Definition}}$$

$$= \underbrace{\mathbf{D}^{el} + \mathbf{D}^{pl}}_{\text{hypo-elastoplastic assumption}}$$

$$\underbrace{\rho\frac{d\mathbf{u}}{dt}}_{m\times a} = \underbrace{\nabla\cdot\sigma}_{\text{Net force}}$$

Shear Transformation Zone Theory

$$\underbrace{\mathbf{D}^{pl}}_{\text{Plastic rate}} = \underbrace{D^{pl} f(\sigma)}_{\propto \text{ deviatoric}}$$

$$\underbrace{\frac{d\chi}{dt}}_{\text{Advective rate}} = \overbrace{\frac{D^{pl}\bar{s}}{s_y c_0}(\chi_\infty - \chi)}^{\text{Relaxation term}} + \underbrace{l^2\nabla\cdot(D^{pl}\nabla\chi)}_{\text{Diffusive term}}$$

Continuum theory

Linear Elasticity

$$\underbrace{\frac{\mathcal{D}\sigma}{\mathcal{D}t}}_{\text{Truesdell Rate}} = \overbrace{\mathbf{C}}^{\text{Stiffness}} : \underbrace{\mathbf{D}^{\text{el}}}_{\text{Elastic Part}}$$

$$\underbrace{\mathbf{D}}_{\text{Rate of deformation}} = \underbrace{\frac{1}{2}(\nabla\mathbf{u} + (\nabla\mathbf{u})^T)}_{\text{Definition}}$$

$$= \underbrace{\mathbf{D}^{el} + \mathbf{D}^{pl}}_{\text{hypo-elastoplastic assumption}}$$

$$\underbrace{\rho\frac{d\mathbf{u}}{dt}}_{m\times a} = \underbrace{\nabla\cdot\sigma}_{\text{Net force}}$$

Shear Transformation Zone Theory

$$\underbrace{\mathbf{D}^{pl}}_{\text{Plastic rate}} = D^{pl}\underbrace{f(\sigma)}_{\propto\ \text{deviatoric}}$$

$$\underbrace{\frac{d\chi}{dt}}_{\text{Advective rate}} = \overbrace{\frac{D^{pl}\bar{s}}{s_y c_0}(\chi_\infty - \chi)}^{\text{Relaxation term}} + \underbrace{l^2\nabla\cdot(D^{pl}\nabla\chi)}_{\text{Diffusive term}}$$

$$D^{\text{pl}} \propto (\text{Density of STZs}) \times (\text{Arrhenius barrier crossing})$$
$$\times\ (\text{Rates for forward and reverse transitions}) \times \left(1 - \frac{s_y}{\bar{s}}\right)$$
$$\times \begin{cases} 1 & \text{if local stress above yield stress} \\ 0 & \text{else} \end{cases}$$

The quasi-static and incompressible limits

Hypo-elastoplastic long-time limit

Incompressible limit of Navier-Stokes

From Navier-Stokes to hypo-elastoplasticity

The quasi-static and incompressible limits

Hypo-elastoplastic long-time limit

$$\underbrace{\frac{\mathcal{D}\sigma}{\mathcal{D}t} = \mathbf{C} : (\mathbf{D} - \mathbf{D}^{\mathsf{pl}})}_{\text{hypo-elastoplastic equation}}$$

Incompressible limit of Navier-Stokes

From Navier-Stokes to hypo-elastoplasticity

The quasi-static and incompressible limits

Hypo-elastoplastic long-time limit

$$\underbrace{\frac{\mathcal{D}\sigma}{\mathcal{D}t} = \mathbf{C} : (\mathbf{D} - \mathbf{D}^{\mathsf{pl}})}_{\text{hypo-elastoplastic equation}}$$

$$\underbrace{\nabla \cdot \sigma \approx 0}_{\text{Quasi-static constraint}}$$

Incompressible limit of Navier-Stokes

From Navier-Stokes to hypo-elastoplasticity

The quasi-static and incompressible limits

Hypo-elastoplastic long-time limit

$$\underbrace{\frac{\mathcal{D}\sigma}{\mathcal{D}t} = \mathbf{C} : (\mathbf{D} - \mathbf{D}^{\mathsf{pl}})}_{\text{hypo-elastoplastic equation}}$$

$$\underbrace{\nabla \cdot \sigma \approx 0}_{\text{Quasi-static constraint}}$$

Incompressible limit of Navier-Stokes

$$\underbrace{\rho \frac{d\mathbf{v}}{dt} = -\nabla p + \nabla \cdot \mathbf{T}}_{\text{Navier-Stokes equation}}$$

From Navier-Stokes to hypo-elastoplasticity

The quasi-static and incompressible limits

Hypo-elastoplastic long-time limit

$$\underbrace{\frac{\mathcal{D}\sigma}{\mathcal{D}t} = \mathbf{C} : (\mathbf{D} - \mathbf{D}^{\mathsf{pl}})}_{\text{hypo-elastoplastic equation}}$$

$$\underbrace{\nabla \cdot \sigma \approx 0}_{\text{Quasi-static constraint}}$$

Incompressible limit of Navier-Stokes

$$\underbrace{\rho \frac{d\mathbf{v}}{dt} = -\nabla p + \nabla \cdot \mathbf{T}}_{\text{Navier-Stokes equation}}$$

$$\underbrace{\nabla \cdot \mathbf{v} \approx 0}_{\text{Incompressibility constraint}}$$

From Navier-Stokes to hypo-elastoplasticity

The quasi-static and incompressible limits

Hypo-elastoplastic long-time limit

$$\underbrace{\frac{\mathcal{D}\sigma}{\mathcal{D}t} = \mathbf{C} : (\mathbf{D} - \mathbf{D}^{\mathrm{pl}})}_{\text{hypo-elastoplastic equation}}$$

$$\underbrace{\nabla \cdot \sigma \approx 0}_{\text{Quasi-static constraint}}$$

Incompressible limit of Navier-Stokes

$$\underbrace{\rho \frac{d\mathbf{v}}{dt} = -\nabla p + \nabla \cdot \mathbf{T}}_{\text{Navier-Stokes equation}}$$

$$\underbrace{\nabla \cdot \mathbf{v} \approx 0}_{\text{Incompressibility constraint}}$$

From Navier-Stokes to hypo-elastoplasticity

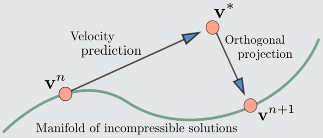

The quasi-static and incompressible limits

Hypo-elastoplastic long-time limit

$$\underbrace{\frac{\mathcal{D}\sigma}{\mathcal{D}t} = \mathbf{C} : (\mathbf{D} - \mathbf{D}^{\text{pl}})}_{\text{hypo-elastoplastic equation}}$$

$$\underbrace{\nabla \cdot \sigma \approx 0}_{\text{Quasi-static constraint}}$$

Incompressible limit of Navier-Stokes

$$\underbrace{\rho \frac{d\mathbf{v}}{dt} = -\nabla p + \nabla \cdot \mathbf{T}}_{\text{Navier-Stokes equation}}$$

$$\underbrace{\nabla \cdot \mathbf{v} \approx 0}_{\text{Incompressibility constraint}}$$

From Navier-Stokes to hypo-elastoplasticity

$$\sigma_{\text{H.E.P.}} \iff \mathbf{v}_{\text{N.S.}}$$

$$\mathbf{u}_{\text{H.E.P.}} \iff p_{\text{N.S.}}$$

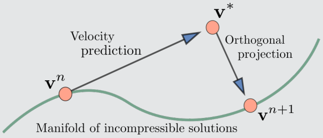

The quasi-static and incompressible limits

Hypo-elastoplastic long-time limit

$$\underbrace{\frac{\mathcal{D}\sigma}{\mathcal{D}t} = \mathbf{C} : (\mathbf{D} - \mathbf{D}^{\mathsf{pl}})}_{\text{hypo-elastoplastic equation}}$$

$$\underbrace{\nabla \cdot \sigma \approx 0}_{\text{Quasi-static constraint}}$$

Incompressible limit of Navier-Stokes

$$\underbrace{\rho \frac{d\mathbf{v}}{dt} = -\nabla p + \nabla \cdot \mathbf{T}}_{\text{Navier-Stokes equation}}$$

$$\underbrace{\nabla \cdot \mathbf{v} \approx 0}_{\text{Incompressibility constraint}}$$

From Navier-Stokes to hypo-elastoplasticity

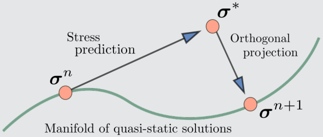

$$\sigma_{\text{H.E.P.}} \iff \mathbf{v}_{\text{N.S.}}$$

$$\mathbf{u}_{\text{H.E.P.}} \iff p_{\text{N.S.}}$$

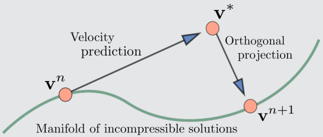

The quasi-static and incompressible limits

Hypo-elastoplastic long-time limit

$$\underbrace{\frac{\mathcal{D}\sigma}{\mathcal{D}t} = \mathbf{C} : (\mathbf{D} - \mathbf{D}^{\mathrm{pl}})}_{\text{hypo-elastoplastic equation}}$$

$$\underbrace{\nabla \cdot \sigma \approx 0}_{\text{Quasi-static constraint}}$$

Incompressible limit of Navier-Stokes

$$\underbrace{\rho \frac{d\mathbf{v}}{dt} = -\nabla p + \nabla \cdot \mathbf{T}}_{\text{Navier-Stokes equation}}$$

$$\underbrace{\nabla \cdot \mathbf{v} \approx 0}_{\text{Incompressibility constraint}}$$

From Navier-Stokes to hypo-elastoplasticity

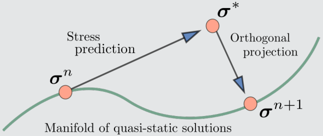

$$\sigma_{\text{H.E.P.}} \iff \mathbf{v}_{\text{N.S.}}$$

$$\mathbf{u}_{\text{H.E.P.}} \iff p_{\text{N.S.}}$$

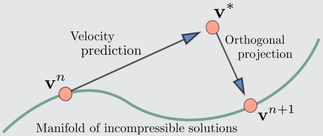

- Any algorithm for Navier-Stokes should work for hypo-elastoplasticity.
- This analogy is independent of the plasticity model.

A quasi-static projection method

A quasi-static projection method

Hypo-elastoplastic equation

- Continuous-time:

$$\frac{\mathcal{D}\sigma}{\mathcal{D}t} = \mathbf{C} : \left(\mathbf{D} - \mathbf{D}^{\mathsf{pl}}\right).$$

- Semi-implicit Euler discretization:

$$\frac{\sigma^{n+1} - \sigma^{n}}{\Delta t} = \left(\frac{D\sigma}{Dt}\right)^{n} - \left(\mathbf{C} : \mathbf{D}^{\mathsf{pl}}\right)^{n} + \left(\mathbf{C} : \mathbf{D}\right)^{n+1}$$

A quasi-static projection method

Hypo-elastoplastic equation

- Continuous-time:

$$\frac{\mathcal{D}\sigma}{\mathcal{D}t} = \mathbf{C} : \left(\mathbf{D} - \mathbf{D}^{\mathsf{pl}}\right).$$

- Semi-implicit Euler discretization:

$$\frac{\sigma^{n+1} - \sigma^{n}}{\Delta t} = \left(\frac{D\sigma}{Dt}\right)^{n} - \left(\mathbf{C} : \mathbf{D}^{\mathsf{pl}}\right)^{n} + \left(\mathbf{C} : \mathbf{D}\right)^{n+1}$$

Advection step

- Just drop the $\mathbf{C} : \mathbf{D}$ term!

$$\frac{\sigma^{*} - \sigma^{n}}{\Delta t} = \left(\frac{D\sigma}{Dt}\right)^{n} - \left(\mathbf{C} : \mathbf{D}^{\mathsf{pl}}\right)^{n}$$

- Parallelized using domain decomposition and MPI (along with χ update).
- Solved on a staggered grid with σ and χ at cell centers and $\mathbf{u}$ at cell corners.

A quasi-static projection method

Hypo-elastoplastic equation

- Continuous-time:

$$\frac{\mathcal{D}\sigma}{\mathcal{D}t} = \mathbf{C} : \left(\mathbf{D} - \mathbf{D}^{\mathsf{pl}}\right).$$

- Semi-implicit Euler discretization:

$$\frac{\sigma^{n+1} - \sigma^n}{\Delta t} = \left(\frac{D\sigma}{Dt}\right)^n - \left(\mathbf{C} : \mathbf{D}^{\mathsf{pl}}\right)^n + \left(\mathbf{C} : \mathbf{D}\right)^{n+1}$$

Advection step

- Just drop the $\mathbf{C} : \mathbf{D}$ term!

$$\frac{\sigma^* - \sigma^n}{\Delta t} = \left(\frac{D\sigma}{Dt}\right)^n - \left(\mathbf{C} : \mathbf{D}^{\mathsf{pl}}\right)^n$$

- Parallelized using domain decomposition and MPI (along with χ update).
- Solved on a staggered grid with σ and χ at cell centers and $\mathbf{u}$ at cell corners.

Projection step

- σ^{n+1} can be computed from σ^* just by adding back in the $\mathbf{C} : \mathbf{D}$ term.

$$\frac{\sigma^{n+1} - \sigma^*}{\Delta t} = \mathbf{C} : \mathbf{D}^{n+1}$$

A quasi-static projection method

Hypo-elastoplastic equation

- Continuous-time:

$$\frac{\mathcal{D}\sigma}{\mathcal{D}t} = \mathbf{C} : \left(\mathbf{D} - \mathbf{D}^{\mathrm{pl}}\right).$$

- Semi-implicit Euler discretization:

$$\frac{\sigma^{n+1} - \sigma^n}{\Delta t} = \left(\frac{D\sigma}{Dt}\right)^n - \left(\mathbf{C} : \mathbf{D}^{\mathrm{pl}}\right)^n + \left(\mathbf{C} : \mathbf{D}\right)^{n+1}$$

Advection step

- Just drop the $\mathbf{C} : \mathbf{D}$ term!

$$\frac{\sigma^* - \sigma^n}{\Delta t} = \left(\frac{D\sigma}{Dt}\right)^n - \left(\mathbf{C} : \mathbf{D}^{\mathrm{pl}}\right)^n$$

- Parallelized using domain decomposition and MPI (along with χ update).
- Solved on a staggered grid with σ and χ at cell centers and $\mathbf{u}$ at cell corners.

Projection step

- σ^{n+1} can be computed from σ^* just by adding back in the $\mathbf{C} : \mathbf{D}$ term.

$$\frac{\sigma^{n+1} - \sigma^*}{\Delta t} = \mathbf{C} : \mathbf{D}^{n+1}$$

Linear system for the velocity

- Take divergence of the projection step:

$$\nabla \cdot \sigma^* = -\Delta t \nabla \cdot \left(\mathbf{C} : \mathbf{D}^{n+1}\right)$$

- Solved using a custom C++ implementation of the geometric multigrid method.
- Implementation is parallelized using MPI and interfaces with the advection step.
- Optimal MPI decomposition computed at each level.
- C++ templates to solve for an arbitrary datatype at each point in space - in this case, a 3-vector.

Simulation methods for BMGs

Molecular Dynamics

Continuum-Scale

Simulation methods for BMGs

Molecular Dynamics

- Physically exact up to integration errors and choice of atomic potentials.

Continuum-Scale

- Requires constitutive equations and a phenomenological plasticity model.

Simulation methods for BMGs

Molecular Dynamics

- Physically exact up to integration errors and choice of atomic potentials.
- Complete information about atomic structure and atomic configurations.

Continuum-Scale

- Requires constitutive equations and a phenomenological plasticity model.
- Fine-scale details have been coarse-grained into internal model variables.

Simulation methods for BMGs

Molecular Dynamics

- Physically exact up to integration errors and choice of atomic potentials.
- Complete information about atomic structure and atomic configurations.
- Computationally expensive!

Continuum-Scale

- Requires constitutive equations and a phenomenological plasticity model.
- Fine-scale details have been coarse-grained into internal model variables.
- Fast, scalable simulation.

Simulation methods for BMGs

Molecular Dynamics

- Physically exact up to integration errors and choice of atomic potentials.
- Complete information about atomic structure and atomic configurations.
- Computationally expensive!
- Typically employs Lees-Edwards boundary conditions.

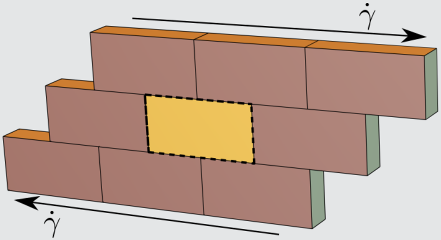

Continuum-Scale

- Requires constitutive equations and a phenomenological plasticity model.
- Fine-scale details have been coarse-grained into internal model variables.
- Fast, scalable simulation.

Simulation methods for BMGs

Molecular Dynamics

- Physically exact up to integration errors and choice of atomic potentials.
- Complete information about atomic structure and atomic configurations.
- Computationally expensive!
- Typically employs Lees-Edwards boundary conditions.

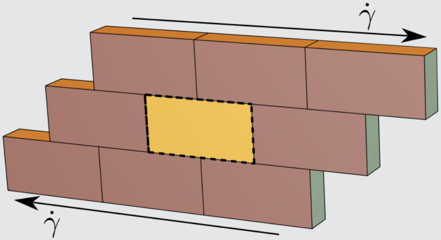

Continuum-Scale

- Requires constitutive equations and a phenomenological plasticity model.
- Fine-scale details have been coarse-grained into internal model variables.
- Fast, scalable simulation.
- Typically employs parallel-plate boundary conditions.

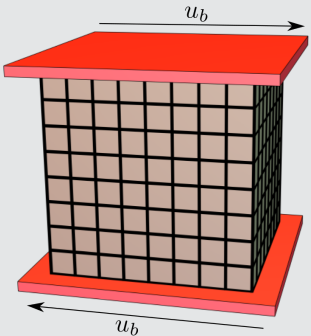

Transformation methodology

Transformation methodology

- Reference or *transformed* domain with coordinate $\mathbf{X}$.
- Physical, deformed domain with coordinate $\mathbf{x}$.

Transformation methodology

- Reference or *transformed* domain with coordinate $\mathbf{X}$.
- Physical, deformed domain with coordinate $\mathbf{x}$.
- Linear time-dependent mapping $\mathbf{T}(t)$ *defines the physical situation*.

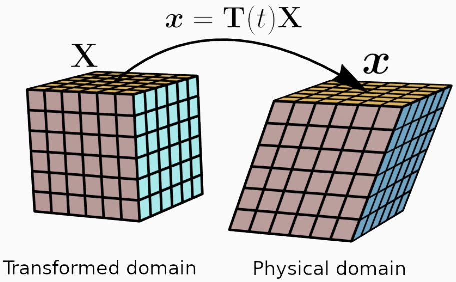

Transformation methodology

- Reference or *transformed* domain with coordinate $\mathbf{X}$.
- Physical, deformed domain with coordinate $\mathbf{x}$.
- Linear time-dependent mapping $\mathbf{T}(t)$ *defines the physical situation*.
- Define the transformed velocity and stress:

$$\mathbf{V} = \mathbf{T}^{-1}\left(\mathbf{v} - \frac{\partial \mathbf{T}}{\partial t}\mathbf{X}\right)$$
$$\Sigma = \mathbf{T}^{-1}\sigma\mathbf{T}^{-T}$$

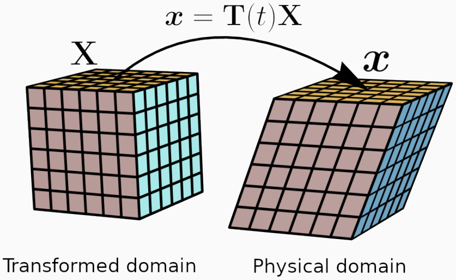

- Reference or *transformed* domain with coordinate $\mathbf{X}$.
- Physical, deformed domain with coordinate $\mathbf{x}$.
- Linear time-dependent mapping $\mathbf{T}(t)$ *defines the physical situation*.
- Define the transformed velocity and stress:

$$\mathbf{V} = \mathbf{T}^{-1}\left(\mathbf{v} - \tfrac{\partial \mathbf{T}}{\partial t}\mathbf{X}\right)$$
$$\Sigma = \mathbf{T}^{-1}\sigma\mathbf{T}^{-T}$$

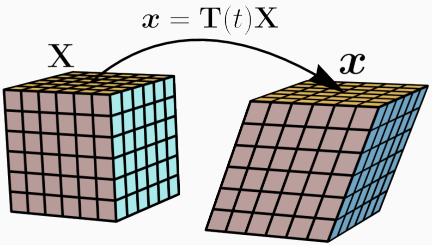

Transformed Evolution Equations

$$\frac{\partial \Sigma}{\partial t} = -\left(\mathbf{V}\cdot\nabla_{\mathbf{X}}\right)\Sigma - \operatorname{tr}(\mathbf{L})\Sigma + \Sigma\left(\mathbf{T}^{\mathsf{T}}\mathbf{L}^{\mathsf{T}}\mathbf{T}^{-\mathsf{T}}\right) + \left(\mathbf{T}^{-1}\mathbf{L}\mathbf{T}\right)\Sigma$$
$$+\,\mathbf{T}^{-1}\left(\mathbf{C} : \left(\mathbf{D} - \mathbf{D}^{\mathrm{pl}}\right) - \frac{\partial \mathbf{T}}{\partial t}\Sigma\mathbf{T}^{\mathsf{T}} - \mathbf{T}\Sigma\frac{\partial \mathbf{T}^{\mathsf{T}}}{\partial t}\right)\mathbf{T}^{-\mathsf{T}}.$$

$$\frac{\partial \mathbf{V}}{\partial t} = -\left(\mathbf{V}\cdot\nabla_{\mathbf{X}}\right)\mathbf{V} + \frac{\partial \mathbf{T}^{-1}}{\partial t}\mathbf{T}\mathbf{V} + \mathbf{T}^{-1}\left(\mathbf{T}^{-\mathsf{T}}\nabla_{\mathbf{X}}\cdot\left(\mathbf{T}\Sigma\mathbf{T}^{\mathsf{T}}\right) - \frac{\partial^2 \mathbf{T}}{\partial t^2}\mathbf{X} - \frac{\partial \mathbf{T}}{\partial t}\mathbf{V}\right).$$

Quasi-static shear simulations

N. M. Boffi & C. H. Rycroft. Parallel three-dimensional simulations of quasi-static elastoplastic solids. Part I: Numerical formulation and examples. 2019. arXiv e-prints.

N. M. Boffi & C. H. Rycroft. Parallel three-dimensional simulations of quasi-static elastoplastic solids. Part II: Coordinate transformations. 2019. arXiv e-prints.

Quasi-static shear simulations

- $512 \times 512 \times 256$ grid.
- $\approx 67,000,000$ grid points in the bulk.
- Linear system matrix contains $\approx 67,000,000^2$ elements.

N. M. Boffi & C. H. Rycroft. Parallel three-dimensional simulations of quasi-static elastoplastic solids. Part I: Numerical formulation and examples. 2019. arXiv e-prints.

N. M. Boffi & C. H. Rycroft. Parallel three-dimensional simulations of quasi-static elastoplastic solids. Part II: Coordinate transformations. 2019. arXiv e-prints.

Quasi-static shear simulations

- $512 \times 512 \times 256$ grid.
- $\approx 67,000,000$ grid points in the bulk.
- Linear system matrix contains $\approx 67,000,000^2$ elements.
- Normally distributed initial χ field at each grid point $\chi_0(i,j,k) \sim N(\mu,\sigma)$.

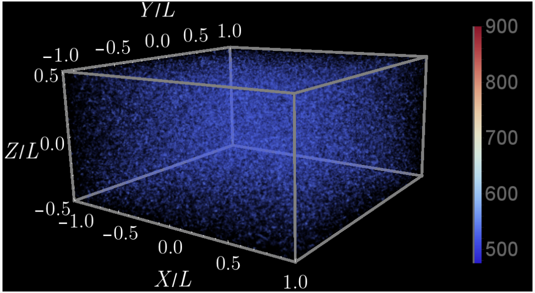

N. M. Boffi & C. H. Rycroft. Parallel three-dimensional simulations of quasi-static elastoplastic solids. Part I: Numerical formulation and examples. 2019. arXiv e-prints.

N. M. Boffi & C. H. Rycroft. Parallel three-dimensional simulations of quasi-static elastoplastic solids. Part II: Coordinate transformations. 2019. arXiv e-prints.

Quasi-static shear simulations

- $512 \times 512 \times 256$ grid.
- $\approx 67,000,000$ grid points in the bulk.
- Linear system matrix contains $\approx 67,000,000^2$ elements.
- Normally distributed initial χ field at each grid point $\chi_0(i,j,k) \sim N(\mu,\sigma)$.
- Basic projection: parallel plate boundary conditions: specify $u = U_b$ on top boundary and $u = -U_b$ on bottom.

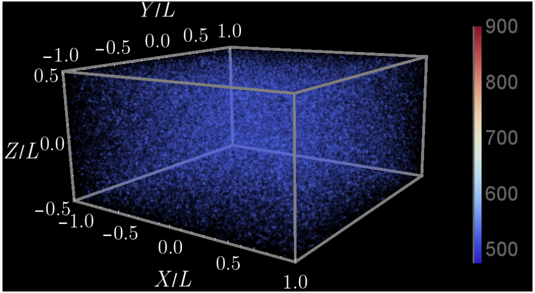

N. M. Boffi & C. H. Rycroft. Parallel three-dimensional simulations of quasi-static elastoplastic solids. Part I: Numerical formulation and examples. 2019. arXiv e-prints.

N. M. Boffi & C. H. Rycroft. Parallel three-dimensional simulations of quasi-static elastoplastic solids. Part II: Coordinate transformations. 2019. arXiv e-prints.

Quasi-static shear simulations

- $512 \times 512 \times 256$ grid.
- $\approx 67,000,000$ grid points in the bulk.
- Linear system matrix contains $\approx 67,000,000^2$ elements.
- Normally distributed initial χ field at each grid point $\chi_0(i,j,k) \sim N(\mu, \sigma)$.
- Basic projection: parallel plate boundary conditions: specify $u = U_b$ on top boundary and $u = -U_b$ on bottom.

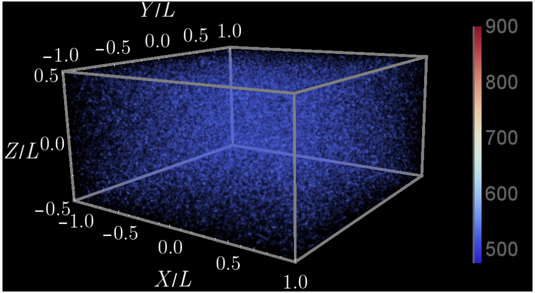

Simple Shear
$$\mathbf{T}(t) = \begin{pmatrix} 1 & 0 & u_b t \\ 0 & 1 & 0 \\ 0 & 0 & 1 \end{pmatrix}$$

Pure Shear
$$\mathbf{T}(t) = \begin{pmatrix} e^{\zeta t} & 0 & 0 \\ 0 & 1 & 0 \\ 0 & 0 & e^{-\zeta t} \end{pmatrix}$$

N. M. Boffi & C. H. Rycroft. Parallel three-dimensional simulations of quasi-static elastoplastic solids. Part I: Numerical formulation and examples. 2019. arXiv e-prints.

N. M. Boffi & C. H. Rycroft. Parallel three-dimensional simulations of quasi-static elastoplastic solids. Part II: Coordinate transformations. 2019. arXiv e-prints.

Quasi-static shear simulations

- $512 \times 512 \times 256$ grid.
- $\approx 67,000,000$ grid points in the bulk.
- Linear system matrix contains $\approx 67,000,000^2$ elements.
- Normally distributed initial χ field at each grid point $\chi_0(i,j,k) \sim N(\mu,\sigma)$.
- Basic projection: parallel plate boundary conditions: specify $u = U_b$ on top boundary and $u = -U_b$ on bottom.
- ≈ 4 day simulation time with 32 threads.

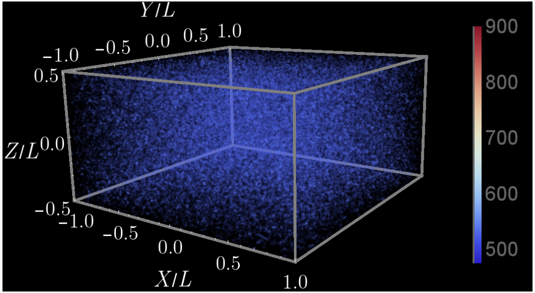

Simple Shear
$$\mathbf{T}(t) = \begin{pmatrix} 1 & 0 & u_b t \\ 0 & 1 & 0 \\ 0 & 0 & 1 \end{pmatrix}$$

Pure Shear
$$\mathbf{T}(t) = \begin{pmatrix} e^{\zeta t} & 0 & 0 \\ 0 & 1 & 0 \\ 0 & 0 & e^{-\zeta t} \end{pmatrix}$$

N. M. Boffi & C. H. Rycroft. Parallel three-dimensional simulations of quasi-static elastoplastic solids. Part I: Numerical formulation and examples. 2019. arXiv e-prints.

N. M. Boffi & C. H. Rycroft. Parallel three-dimensional simulations of quasi-static elastoplastic solids. Part II: Coordinate transformations. 2019. arXiv e-prints.

Conclusions, Future Directions, and Acknowledgments

- Metallic glasses are a promising class of materials limited by shear banding.
- Quasi-static projection algorithm enables simulation of large systems at long timescales by exploiting an analogy to the incompressible Navier-Stokes equations.
- Transformation methodology enables connection between MD and continuum.

Conclusions, Future Directions, and Acknowledgments

- Metallic glasses are a promising class of materials limited by shear banding.
- Quasi-static projection algorithm enables simulation of large systems at long timescales by exploiting an analogy to the incompressible Navier-Stokes equations.
- Transformation methodology enables connection between MD and continuum.
- Future directions:
  - Extension of transformation methodology to state-dependent case for study of necking.
  - Statistical matching between MD and continuum for prediction of effective temperature from MD configuration.

Conclusions, Future Directions, and Acknowledgments

- Metallic glasses are a promising class of materials limited by shear banding.
- Quasi-static projection algorithm enables simulation of large systems at long timescales by exploiting an analogy to the incompressible Navier-Stokes equations.
- Transformation methodology enables connection between MD and continuum.
- Future directions:
  - Extension of transformation methodology to state-dependent case for study of necking.
  - Statistical matching between MD and continuum for prediction of effective temperature from MD configuration.




DOE CSGF